

# Probing the superconducting condensate on a nanometer scale

Th. Proslir, A. Kohen, Y. Noat, T. Cren, D. Roditchev and W. Sacks

Institut des Nano-Sciences de Paris, IN .S.P., Universit   Paris 6 et Paris 7, et C.N.R.S.  
(UMR 7588), 140 rue de Lourmel, Campus Boucicaut, 75015 Paris, France

PACS.74.50.+r { First pacs description.

PACS.74.70.-b { Second pacs description.

PACS.07.79.Cz { Third pacs description.

## Abstract.

Superconductivity is a rare example of a quantum system in which the wavefunction has a macroscopic quantum effect, due to the unique condensate of electron pairs. The amplitude of the wavefunction is directly related to the pair density, but both amplitude and phase enter the Josephson current: the coherent tunneling of pairs between superconductors. Very sensitive devices exploit the superconducting state, however properties of the condensate on the local scale are largely unknown, for instance, in unconventional high- $T_c$  cuprate, multiple gap, and gapless superconductors.

The technique of choice would be Josephson STS, based on Scanning Tunneling Spectroscopy (STS), where the condensate is directly probed by measuring the local Josephson current (JC) between a superconducting tip and sample. However, Josephson STS is an experimental challenge since it requires stable superconducting tips, and tunneling conditions close to atomic contact. We demonstrate how these difficulties can be overcome and present the first spatial mapping of the JC on the nanometer scale. The case of an MgB<sub>2</sub> film, subject to a normal magnetic field, is considered.

Introduction. { As Landau first suggested, the superconducting (SC) state is a quantum condensate represented by a macroscopic wavefunction  $\Psi = \Psi_0 e^{i\phi}$ , accounting for the two fundamental properties: zero resistance and perfect diamagnetism. This SC wavefunction varies on the scale of the coherence length  $\xi$ : when the superconductor is in contact with a normal metal, or within the vortex core. However, up to present, local variations of the SC state have not been measured in a direct way, but rather inferred indirectly.

Local electronic properties are probed by scanning tunneling microscopy/spectroscopy (STM/STS), where the tunneling current between an atomically sharp tip and a sample as a function of the bias voltage,  $I(V)$ , is measured. Atomic or larger-scale images of the surface can be done by scanning the tip (topographic mode), or at a given point,  $I(V)$  curves are locally acquired (spectroscopic mode). Usually the tip is made of a normal metal (W or Pt/Ir) whose density of states (DOS) near the Fermi level is roughly constant. Then the differential conductance,  $dI/dV$ , is proportional to the sample local DOS (at the energy  $E_F + eV$ ).

An important advance is STS: the combination of topographic imaging with tunneling spectroscopy, resulting in high resolution conductance maps (equivalently DOS maps). Using a normal metal tip to study superconductors, STS measures the quasiparticle (QP) DOS, first derived by Bardeen, Cooper and Schrieffer, which generally reveals a gap  $\Delta$  at the Fermi level. Giaever [1] verified the BCS model using planar junctions in which a thin oxide layer separates a normal metal electrode from a superconducting one (SIN junction) or two

superconductors (SIS junction). In their pioneering work, Hess et al. [2,3] extensively studied the Abrikosov vortex lattice in  $2H\text{-NbSe}_2$ , in a magnetic field, using low temperature STS. However, there one observes the changes of the quasiparticle DOS due to the suppression of the gap in the vortex cores; it is not a direct measurement of the condensate.

Measuring the SC condensate is particularly needed in the case of high- $T_c$  cuprates, where the microscopic mechanism is still unknown. STS conductance mapping has shown that a pseudogap at the Fermi level, existing within the vortex core [4], is also induced by disorder [5(8)] with a shape similar to the one found above  $T_c$ . Thus, the origin of this pseudogap is a key question [9] and the quasiparticle DOS measurement alone cannot decide on its physical origin. The QP spectrum does not suffice for gapless superconductivity, where the conductance gap is locally vanishing due to supercurrents or magnetic impurities, while a condensate exists. A direct probe of the Cooper pair density is therefore needed.

As predicted by Josephson [10] in 1962, and first verified by Anderson and Rowell [11], a distinct current can flow between two superconductors separated by a thin layer: the tunneling of Cooper pairs. The Josephson current (JC) is a supercurrent due to the phase difference between the SC wavefunctions of the electrodes, allowing a DC flow for zero bias voltage across the junction. The Josephson effect is not only the basis of very sensitive and fast switching devices, but it is the measurable quantity directly connected to the quantum condensate. Recently two groups [12,13] have been able to measure the JC using low temperature STM, but only at a single point. In this Letter we report the first mapping of the Josephson current, using a superconducting  $\text{MgB}_2$  tip as a novel STS probe.

Towards Josephson spectroscopy. { The first step towards a Josephson STM is to realize stable SC tips showing characteristic spectra both in the SIN (normal surface) or SIS (superconductor surface) cases. In the former, the observed conductance gap is just 2 , while in the SIS configuration, it is  $2(\epsilon_{\text{tip}} + \epsilon_{\text{sample}})$ , see Fig.1. In comparison, the SIS singularities are very sharp, due to the convolution of the tip and sample DOS. A second set of peaks, for finite  $T$ , are characteristic of the SIS junction and occur at  $(\epsilon_{\text{tip}} - \epsilon_{\text{sample}})$ ; see right inset of Fig.1. Pan et al. [14] showed both SIN and SIS tunneling using a Nb tip, while later Naaman [12] and Rodrigo [13] et al. used Pb tips, or Pb covered in a thin layer of Ag. Our results in Fig.1 are very similar to these works.

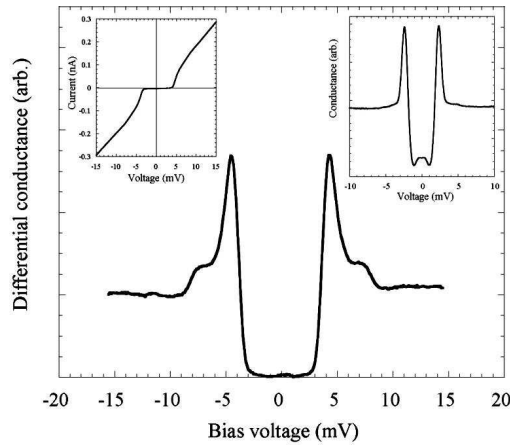


Fig.1. SIS conductance and I-V (Left Inset) curves, taken at  $T = 2\text{ K}$ , using a single crystal  $\text{MgB}_2$  tip and an  $\text{MgB}_2$  sample. Right Inset: Conductance spectrum for Nb tip/ $\text{NbSe}_2$  sample ( $T = 4.2\text{ K}$ ).

We produce SC tips with two methods, either by mechanically breaking a Nb wire in the STM vacuum chamber [15], or by gluing a small  $\text{MgB}_2$  single crystal to a PtIr wire [16]. Both procedures yield tips having distinctive SC properties, as revealed by SIN and SIS spectroscopy.  $\text{MgB}_2$  is a two-band superconductor [16,17] offering different signatures in the quasiparticle SIS characteristics, depending on the tip (or sample) surface. If the sample is an  $\text{MgB}_2$  thin film, as in Fig.1, with c axis normal to the film, the small gap dominates

the quasiparticle current: the total conductance gap seen in Fig.1 is then  $4 \times 10$  m eV as expected [18]. The large gap,  $\sim 7$  m eV, gives secondary peaks whose resolution depends on the local tunneling geometry. This is a particular electronic structure effect, since the tunneling into the 3D band has a higher probability than to the 2D band.

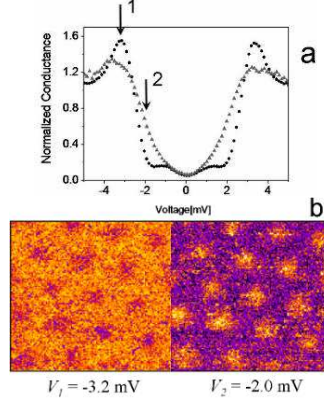


Fig 2. STS scan of the vortices in 2H-NbSe<sub>2</sub> using a superconducting MgB<sub>2</sub> tip. (a) Normalized conductance measured in the vortex core (SIN), triangles, and in between the vortices (SIS), dots. (b) Raw conductance maps at the indicated voltages (1 and 2 in a). Scan range: 380 nm, magnetic field: 0.25 Tesla, Temperature: 4.2 K.

The second step is to realize STS mapping in the SIS configuration. While atomic resolution in the topographic mode has been previously obtained [14-16], to our knowledge scanning spectroscopy has not been achieved with SC tips. However, it is a basic requirement for the Josephson microscopy. Probing the vortex lattice in 2H-NbSe<sub>2</sub>, using either MgB<sub>2</sub> or niobium tips, tests the spatial resolution of the sample DOS and the stability of the tip SC properties in the magnetic field. In Fig 2b we show the vortices, obtained with an MgB<sub>2</sub> tip, clearly revealed in the QP conductance maps at the selected bias voltages:  $V_1$  at the QP peak and  $V_2$  within the conductance gap. The contrast reversal of the maps, for these two voltages, is expected: between the vortices the conductance is of the SIS type, while in the vortex core the junction becomes SIN (see Fig 2a). A complete discussion of the bias-dependant conductance maps, in the SIS geometry with a Nb tip, can be found in [19].

The penultimate step towards Josephson microscopy is to measure the JC systematically throughout the sample. In this regard, the JC measurement is quite different from conventional STS since the probability for pair tunneling is much smaller than for single quasiparticles [20]. Consequently the tunneling resistance must be set much lower, e.g. 50 k $\Omega$ , as compared to the usual 100 M $\Omega$ , maintained high so that the tip never touches the sample. As given by Ambegaokar and Baratoff [21], assuming identical superconductors at  $T = 0$ , the  $I_c R_n$  product is:  $I_c R_n = \frac{1}{2} e^2$  where  $R_n$  is the normal (QP) resistance. The Josephson coupling energy,  $E_J = (\hbar/2e) I_c$  must be larger than  $kT$ , or else thermal smearing prevents the effect. Then one has the condition:

$$R_n < \frac{\hbar}{2e^2 kT} R_0$$

where  $R_0$  is the quantum resistance ( $\hbar/e^2$ ). As pointed out by Smakov et al. [20], with usual values of the gap and  $T$ , it is quite difficult to measure the JC without requiring direct contact between tip and sample:  $R_n$  is close to  $R_0$ . In the remainder of this work we use MgB<sub>2</sub> tips, where the JC is stronger than for Nb, for which one estimates, at  $T = 2$  K,  $R_n < 60$  k $\Omega$ .

Namian, Teizer and Dynes [12] have measured the JC, using Pb/Ag tips on a Pb sample, in the case where the above inequality is only roughly verified: the result is unambiguous pair tunneling. Indeed, Ivanchenko et al. [22] have shown that the JC for very small junctions is strongly affected by the fluctuations of the relative phase  $\phi$  between the SC condensates of the two electrodes. For a voltage biased junction, a characteristic  $dI(V)/dV$  curve is obtained, with a sharp peak at zero bias. Our JC measurements using the

MgB<sub>2</sub> tip, Fig. 3, reveal the same qualitative  $I(V)$  and conductance curves as those of Ref. [12]. The spectra were obtained in succession by lowering the normal tunneling resistance  $R_n$  from 31 down to 14 k $\Omega$ , with a final  $I_c R_n$  product of 4 m eV. Raising the resistance again gives back a similar set of  $I(V)$  curves. Based on the theory of [22], and the correct response of the junctions subject to a micro-wave field by Naaman et al. [12], this JC is directly related to the pair density of the sample.

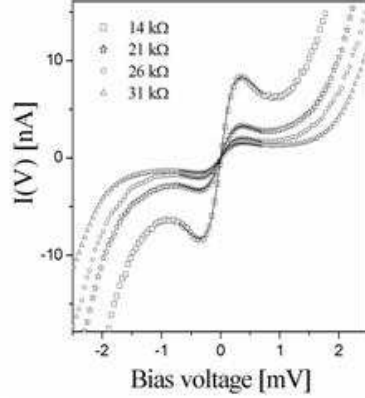


Fig.3.  $I(V)$  spectra for the MgB<sub>2</sub>-MgB<sub>2</sub> junction (STM at a single point,  $T = 2.1$  K). Inset: corresponding tunneling resistance values ( $R_n$ ). Solid line: fit using the theory of [22].

The solid lines in Fig. 3 are the fits using the theory of Ref. [22] in which the phase fluctuations are due to the voltage noise at the junction, represented by an effective temperature  $T_{eff}$ :  $\langle v(t)v(0) \rangle = 2RkT_{eff} \langle \xi(t) \rangle$ , where  $R$  is the source resistance. As part of this noise originates from the STM electronics at 300 K,  $T_{eff}$  can be much higher than the actual temperature of the junction (2.1 K). Using  $\Delta = 2.5$  m eV from the SIS spectra, and knowing  $R_n$ , we deduce from the series of fits:  $T_{eff} = 66$  K and  $R = 100 \Omega$ , close to the values of [12] for a similar electronics:  $T_{eff} = 56$  K and  $R = 80 \Omega$ . This fluctuating voltage  $\sim 50$   $\mu$ V does not affect the QP spectrum, as in Fig. 1, while it strongly does in Fig. 3 (JC) through the phase fluctuations. For superconductors having a small gap compared to MgB<sub>2</sub>, in addition to lower temperature, it may be necessary to further reduce the high-frequency voltage noise reaching the junction. Besides filtering, part of the electronics can be placed at low temperature, on or near the STM. In our case, Fig. 3, the agreement between theory and experiment is satisfactory: the conductance peak measured at zero bias is indeed the fluctuating JC.

Josephson conductance mapping. The first step is to perform scanning while measuring the JC in the STM spectroscopic mode. However, a high resistance is needed during the tip scan, to avoid irreversible tip damage, but a low resistance is needed to measure the JC. We have redesigned our STS acquisition [6] (i.e. a complete I-V spectrum at each pixel of an image) and have developed a new 'sewing needle' scanning mode. In this mode, the tip is approached towards the surface (lower  $V$ , higher  $I$ ) in order to obtain a much smaller resistance (in the 60 k $\Omega$  m range, or less). An I-V spectrum is acquired. The tip is then retracted from the surface (higher  $V$ , lower  $I$ ), moved to the next point of the image, and the cycle is repeated. This 'sewing needle' mode is an essential ingredient of the Josephson STM, where the feedback remains active when lowering and stabilizing the tip prior to acquiring the spectrum. In this way, the complete STS data set consists of 256 JC conductance maps,  $dI = dV(V; x, y)$ , measured simultaneously with the topography. A similar data set is acquired for the QP conductance maps.

We now discuss how the spatial maps of the JC correlate to the QP conductance maps and to the topographic map. Here we consider an MgB<sub>2</sub> thin film, with  $c$  axis oriented normal to the substrate and subject to a magnetic field of 0.18 Tesla, applied normal to the surface. In Fig. 4, the principal results of a complete STS scan over a selected region of the film are summarized. Both Josephson and quasiparticle DOS maps were acquired in this identical

region : 256 images are simultaneously acquired where in the first, the bias voltage range is from  $-2$  to  $+2$  mV, and in the second, from  $-15$  to  $+15$  mV.

The topography is shown in image a revealing six or so different grains. In comparison, the quasiparticle DOS maps are complex and rich in information, with variations of both the conductance gap width and the peak intensity. To simplify the discussion, we display in c a color map of the quasiparticle peak intensity at the selected voltage  $V = -5$  mV, corresponding to the nominal SIS peak of the  $\text{MgB}_2$ - $\text{MgB}_2$  junction (i.e.  $eV = 2$ ). In such a way, a small or smoothed gap appears dark, and a sharp conductance peak appears bright. Analogously, we display in map d the JC conductance peak intensity at zero bias (see f). While the two maps c and d have a different origin (i.e. QP conductance in c and JC in d), they show a definite spatial correlation between them.

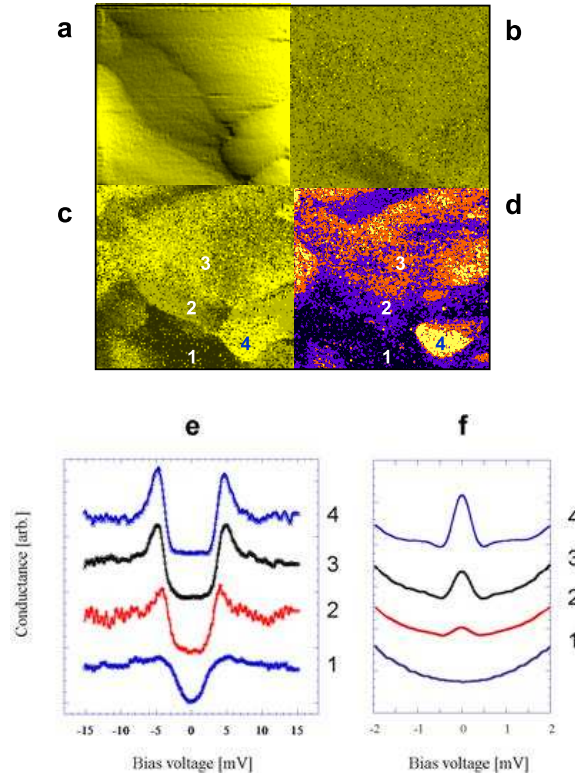


Fig.4. Analysis of a complete STS scan of a  $220 \text{ nm} \times 220 \text{ nm}$  area of the  $\text{MgB}_2$  thin film, and using the  $\text{MgB}_2$  tip, representing a total of  $2 \times 128 \times 128$   $I(V)$  spectra :

- a. The topography (standard STM Z-deflection),
- b. Josephson conductance map at  $V = 2$  mV
- c. Quasiparticle peak intensity map, at  $V = -5$  mV,
- d. Josephson conductance map, at  $V = 0$  mV

Regions 1-4, defined by the colour scale of image d, reveal the characteristic spectra :

- e. Quasiparticle conductance spectra (regions 1-4),
- f. Josephson conductance spectra (regions 1-4)

In e and f the curves are normalized to the same value, then offset for clarity.

The entire scan area ( $220 \text{ nm} \times 220 \text{ nm}$ ) can consequently be divided into regions where the SC state has similar characteristics. Furthermore, by comparison to the topographic image (a), some of the regions can be identified with individual grains. This is not always the case, there are two dark regions, at the lower part and the very upper part of the QP image (c), where the superconducting state is either very weak (upper dark region) or totally absent (lower dark region). In this experiment, as the  $\text{MgB}_2$  film was subject to a normal field, magnetic flux is present at the locations of strong defects, but no vortex lattice is observed.

Furthermore, as will be shown, the spectra acquired within these regions lead to the conclusion that they correspond to a vanishing order parameter.

The complete STS data set allows to select precisely the spectra corresponding to the regions 1-4, as defined in the figure, for direct comparison. The QP conductance and the JC spectra are plotted in Fig.4e and Fig.4f, respectively. It is immediately evident that the general trend of the JC curves follows the trend of the QP curves. The strongest JC peak occurs in region 4, precisely where the SC gap has the most significant SIS characteristics (strongest peaks and deep gap). On the contrary, in region 1, the Josephson peak is totally absent and the QP spectrum is typical of the SIN type, i.e. the pair potential ( $\Delta$ ) is locally vanishing. Regions 2 and 3 are thus intermediate, and they display a less-pronounced Josephson peak, accompanied by weaker SIS characteristics, with a smaller conductance gap. For regions 1-4, the local JC intensity correlates perfectly to the local SIS spectra.

The Josephson conductance map at the selected value of  $V = 2.0$  mV, in Fig.4b, is shown for comparison to the JC map at zero bias, d. A side from the normal region 1 discussed above, there is practically no change in the spatial characteristics (it appears uniform). This is an important experimental verification of the STS: at this particular voltage ( $V = 2.0$  mV), beyond the Josephson peak and at the same time well below the SIS peak, there is no significant spatial variation of the conductance spectra.

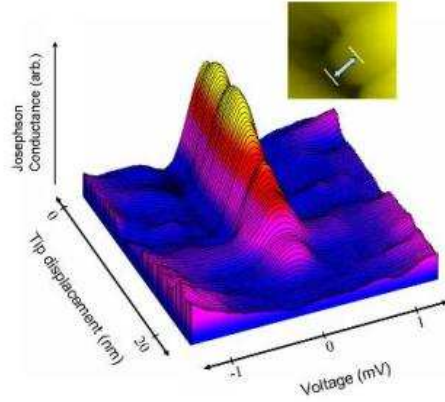


Fig.5. Three-dimensional view of the change in the Josephson conductance peak, as a function of the tip position, along the line (Inset) from region 1 to the center of region 4. The plot is from the identical STS data set of Fig.4. Thus the Josephson current increases from nearly zero to its maximum intensity in a distance of about 15 nm. Inset: Zoom of the topography (from Fig.4a).

Region 4 is of particular interest in that first, it has the highest Josephson conductance peak and second, it correlates to a particular grain observed in the topography. Here the  $I_c R_n$  product is about 4 mV, at its maximum value. We note the variation of the JC as one crosses from the normal region 1 to region 4 across the grain boundary: the change is continuous, but quite abrupt, as shown as a 3D plot in Fig.5. The approximate value for the distance over which the JC peak evolves is 15 nm. Note that the QP conductance follows the shapes 1-4, as in Fig.4e.

The JC peak also decays in the normal region in the upper part of Figs.4c or d, where no particular topographical structure is present. Crossing the entire region along a line, the variation of the JC and the QP conductance shapes are compared in a top-view in Fig.6. Clearly, the JC peak vanishes, on the scale of 25 nm, and reappears again. The parallel effect on the QP spectra, while following the same trend, is less pronounced.

The physical effect is clearly due to the presence of magnetic flux in this region. The evolution of the SIS peaks (right panel of Fig.6) is first the lowering of the peaks due to the supercurrents (Doppler shift) and second, the vanishing of the pair potential, i.e. the junction becomes SIN. We have recently found this precise behavior probing a single vortex with a SC niobium tip [19]. Quantitatively, the coherence length as inferred from the vanishing of

the JC peak in Fig.6,  $\approx 25$  nm, is smaller than the value of Eskildsen et al. [23] ( $\approx 57$  nm) from the DOS crossing the band vortex core, for a single crystal. As  $\text{MgB}_2$  is a two-band superconductor, with a significant coupling between the bands, the effective coherence length depends on the particular experiment and the type of sample (here, a thin film). A lower bound,  $\approx 13$  nm, is estimated from the second critical field,  $H_{c2}$ , while the weak superconductivity of the band gives an upper value of  $\approx 60$  nm.

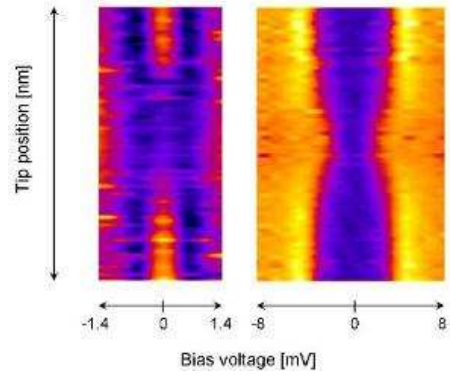


Fig.6. Top-view of the STS scan across the normal zone (upper part of Fig.4c) to compare the JC (left) to the QP (right) variations.

There are also more intricate variations in the Josephson map (4d) as seen in the boundaries of regions 2 and 3. The presence of grain boundaries or impurities may affect the local electronic properties, in addition to the magnetic flux. Due to the coupling between the bands, there could be a contribution to the JC from the Cooper pairs from the band, changing with the (local) tunneling junction. Work is in progress to evaluate this effect but, in a first approximation,  $I_c R_N$  is proportional to the small gap,  $\Delta$ .

The main goal of STS mapping of the JC is therefore achieved. The spatial evolution of the JC is in qualitative agreement with the quasiparticle DOS maps (Fig.4), in a first approximation, which is expected for conventional SC. For the first time the suppression of the SC state, due to the applied magnetic flux, is observed in the JC directly (Fig.6). There is a long list of possible applications of such a probe. It could be used to map the condensate of gapless superconductors, different vortex states, and be of general use in the case of structural changes, such as steps or boundaries, and point defects. It could test the d-wave symmetry of the high- $T_c$  superconductors, with or without these perturbations. Clearly, the origin of the pseudogap is a key question where the observed gap, inferred from the DOS, is not directly the order parameter, and a second energy scale accounts for the transition [9]. A direct probe of the Cooper pair density, such as with the Josephson STS, may help answer the question.

We gratefully thank F. Breton and F. Debontridder for their technical assistance. This work was supported by the project GBP Matériaux aux propriétés remarquables.

## REFERENCES

- [1] I. Giaever, Rev. Mod. Phys. 46, 245 (1974)
- [2] H. F. Hess, R. B. Robinson, R. C. Dynes et al., Phys. Rev. Lett. 62, 214 (1989)
- [3] H. F. Hess, R. B. Robinson, and J. V. Waszczak, Phys. Rev. Lett. 64, 2711 (1990)
- [4] Ch. Renner, B. Revaz, K. Kadowaki, et al. Phys. Rev. Lett. 80, 3606 (1998)
- [5] T. Cren, D. Roditchev, W. Sacks, et al. Phys. Rev. Lett., 84, 1 (2000)
- [6] T. Cren, D. Roditchev, W. Sacks, and J. Klein, Europhys. Lett., 54 (1), 84 (2001)
- [7] S. Pan, J. O'Neal, R. Badzey et al., Nature 413, 282 (2001)
- [8] C. Howald, P. Fournier, and A. Kapitulnik, Phys. Rev. B 64, 100504 (2001)
- [9] G. Deutscher, Nature 397, 410 (1999)
- [10] B. D. Josephson, Phys. Lett., 1, 251 (1962)
- [11] P. W. Anderson and J. M. Rowell, Phys. Rev. Lett. 10, 230 (1963)
- [12] O. Naaman, W. Teizer, and R. C. Dynes, Phys. Rev. Lett. 87, 097004 (2001)

- [13] J. Rodrigo, H. Suderow, and S. Vieira, Eur. Phys. Jour. B, 40, 483 (2004)
- [14] S. H. Pan, E. W. Hudson, and J. C. Davis, Appl. Phys. Lett. 73, 2992 (1998)
- [15] A. Kohen, Y. Noat, T. Proslie et al, Physica C 49, 18 (2005)
- [16] F. G iubileo, D. Roditchev, W. Sacks et al, Phys. Rev. Lett. 87, 177008 (2001)
- [17] S. Souma, Y. Machida, T. Sato et al, Nature 423, 65 (2003)
- [18] F. Bobba, D. Roditchev, R. Lam y et al, Super. Science & Technol, 16, 167 (2003)
- [19] A. Kohen, Th. Proslie, T. Cren, et al, cond-m at 0511699.
- [20] J. Smakov, I. Martin and A. V. Balatsky, Phys. Rev. B. 64, 212506 (2001)
- [21] V. Ambegoakar and A. Barato, Phys. Rev. Lett. 10, 486 (1963)
- [22] M. Ivanchenko and L. A. Zilberm an, Sov. Phys. JETP 28, 1272 (1969).
- [23] M. R. Eskildsen, M. Kugler, S. Tanaka, et al, Phys. Rev. Lett. 89, 187003 (2002)